Melanopsin Signaling in Mammalian Iris and Retina

T. Xue et al.

SUPPLEMENTARY ONLINE INFORMATION

SUPPLEMENTARY METHODS

Generation of *Trpc7*$^{-/-}$ mouse line. *Trpc7*$^{-/-}$ mice were generated by homologous recombination with a targeting construct to delete a region that includes the TATA box upstream of exon 1 and also exon 1 itself, comprising the untranslated region and the start codon. The removal of this region impairs the start of transcription and the synthesis of the TRPC7 protein (Fig. S9a). The targeting construct was linearized and electroporated into embryonic stem (ES) cells derived from 129/SvJ1 mice. G418-resistant colonies were selected and expanded. Southern blotting with probes flanking the targeting-construct sequence detected clones with successful homologous recombination. ES cells harboring the targeting construct were transfected with pOG231, a plasmid for transient Cre expression in order to excise the neomycin cassette and create the KO allele. Subsequent subclones were analyzed by genotyping to obtain those that underwent the appropriate recombination of loxP sites. Chimeric mice were generated by injecting the ES cells into C57BL/6 mouse blastocysts. The chimeric mice were bred with 129/SvImJ mice. The F2 heterozygous mice were backcrossed to 129/SvImJ mice for 8 generations. Mouse-tail genotyping confirmed the disrupted *Trpc7* gene (Fig. S9b). RT–PCR analysis of transcripts from the retina of WT and mutant mice confirmed the absence of *Trpc7* mRNA (Fig. S9c). TRPC7 protein was not detected in *Trpc7*$^{-/-}$ mouse retina by immunoprecipitation (Fig. S9d).

A set of 3 primers was designed for genotyping the mice: F1 was upstream of the first loxP site, R2 was located at the beginning of *Trpc7* intron 1, R3 was located downstream of the second loxP site. The F1 and R2 primers were designed to yield a 388-bp PCR fragment from the WT *mTrpc7* gene; the F1 and R3 primers should amplify an 812-bp PCR fragment from the disrupted targeted *Trpc7* gene (Fig. S9b). Primer sequences were: F1, *5'-CAA CAA GTA GGA AAT CAG CCC ATT C-3'*; R2, *5'-CTT GCC TTC CTG TCC TTT TCC TAA T-3'*, and R3, *5'-CAG ATA CCT GGT TAG CTA CTC CAC TGT G-3'*.

Generation of *Trpc5*$^{-/-}$ mouse line. For construction of the targeting vector (pC5-16b), genomic DNA was isolated from R1 embryonic stem cells and used as template for PCR-amplification of 5' and 3' homology arms with *Pfu* polymerase. The genomic sequence of the 5'-homology arm contained exon 4 of the *Trpc5* gene which was flanked by loxP sites. A splice acceptor (SA)-IRES-GFP cassette, a FRT sequence-flanked pgk-promotor-driven neomycin-resistance gene cassette (neo^r), and a third loxP site was cloned downstream followed by the 3'-homology arm which included exon 5. For negative selection, a herpes simplex virus thymidine kinase cassette (tk) was introduced (Fig. S10a). Embryonic stem (ES) cell culture was essentially done as described[1]. Briefly, R1 ES cells were electroporated with the linearized targeting vector and plated on irradiated G418-resistant embryonic feeder cells isolated from *Trpc4*$^{+/-}$ embryos[2]. Recombinant clones were selected with G418 (0.25 mg/ml) and Ganciclovir (2 μM). Three out of 82 double-resistant colonies showed homologous recombination at the *Trpc5* locus as confirmed by Southern blot hybridization with a 3' probe external to the targeting vector, internal probes and a PCR-based amplification of a genomic DNA fragment specific for the *Trpc5*^{L3F2} allele using a forward primer 5' of the 5'-homology arm (P86: *5'- CTA GGT AAC TGG GAT GTT TAG C- 3'*) and a reverse primer consisting of sequences of the loxP site (P138:

5'-GCT ATA CGA AGT TAT GGT ACC A-3') (Fig. S10d). Germline chimeras obtained by injection of ES cell clones 7B2 and 15A1 into C57BL/6 blastocysts were crossed with C57BL/6N mice to get mice heterozygous for the *Trpc5*^{L3F2} allele (*Trpc5*$^{+/L3F2}$). Mice derived from clone 7B2 were mated with FlpeR (129S4/SvJaeSor-Gt(ROSA)26Sor$^{tm1(FLP1)Dym}$/J) mice[3] to remove the neo cassette and to obtain *Trpc5*$^{+/L3F1}$ mice (Fig. S10b,e) or with the CMV-Cre deleter mouse strain[4] to remove the IRES-GFP and neo^{r} cassettes and to produce mice with a *Trpc5* null allele (*Trpc5* $^{-}$) lacking genomic sequences containing exon 4 (Fig. S10c,f). Mice were routinely genotyped using PCR. Knockout was confirmed by the loss of TRPC5 protein in both brain and retina extracted from *Trpc5*$^{-/-}$ mice (Fig. S10g). All animal experiments were performed in accordance with German legislation on protection of animals and were approved by the local ethics committee.

Animals. The genetically-engineered mouse lines used in this study included: *Plcβ4*$^{-/-}$ (Ref. 5), *Trpc1*$^{-/-}$ (Ref. 6), *Trpc3*$^{-/-}$ (Ref. 7), *Trpc4*$^{-/-}$ (Ref. 1), *Trpc5*$^{-/-}$ (see above), *Trpc6*$^{-/-}$ (Ref. 8), *Trpc7*$^{-/-}$ (see above), *Trpv4*$^{-/-}$ (Ref. 9), *Opn4*$^{-/-}$ (Ref.10), *Cryptochromes-1,2*$^{-/-}$ (Ref. 11), *Rho*$^{-/-}$ (Ref. 12), *Gnat1*$^{-/-}$ (Ref. 13), *cl* (also called *cone-DTA*)[14], and an *Opn4*$^{-/-}$*:tdTomato BAC* transgenic line[15]. *Trpc6,7*$^{-/-}$, *Trpc3,6*$^{-/-}$, *Trpc3,6,7*$^{-/-}$, *Trpc1,4,5*$^{-/-}$, *Gnat1*$^{-/-}$ *cl* and *Gnat1*$^{-/-}$ *cl Opn4*$^{-/-}$ lines were generated by crossing the corresponding lines. *Plcβ4*$^{-/-}$, *Trpc3*$^{-/-}$, *Trpc6*$^{-/-}$, *Trpc7*$^{-/-}$, *Trpc6,7*$^{-/-}$, *Trpc3,6*$^{-/-}$, *Trpc3,6,7*$^{-/-}$ and *Trpc1,4,5*$^{-/-}$ lines were also crossed into the *Opn4*$^{-/-}$*:tdTomato BAC* background in order to identify ipRGCs in single-cell electrophysiological studies. *Opn4*$^{-/-}$ and *Opn4:tdTomato BAC* lines were crossed into a B6 albino background (C57BL/6J-Tyr^{c-2J}/J, Jackson Labs) for immunocytochemistry and tdTomato-fluorescence signal detection. It was not feasible to use WT littermate controls for these complex genotypes, so

C57BL/6J (which was the genetic background for many of the lines) was used instead. Littermate controls were used for experiments on the *Plcβ4*$^{-/-}$ line.

Fresh eyes from rat (Sprague-Dawley), hamster (Syrian hamster, *Mesocricetus auratus*), dog (mongrel), cat (*Felis domesticus*), rabbit (Dutch), pig (Göttingen minipig), guinea pig (English shorthaired), ground squirrel (13-lined ground squirrel), marmoset (*Callithrix jacchus*), rhesus monkey (*Macaca mulatta*), baboon (*Papio papio*) and bush baby (*Galago garnetti*) were obtained from other laboratories in Johns Hopkins University School of Medicine, US National Eye Institute (ground squirrel), Vanderbilt Medical School (bush baby), or Southwest National Primate Research Center, Texas Biomedical Research Institute (baboon). Nile grass rat (*Arvicanthis niloticus*) was a gift from Lauren Smale (Michigan State University), and owl monkey (*Aotus Azarae*) was purchased from MD Anderson Hospital Houston.

Pupillometry of isolated eye. A rapidly enucleated eye from an overnight-dark-adapted mouse was held with ring forceps, video-recorded under infrared illumination, and stimulated with Xe light via a light guide. The experiment was performed at 23^{o}C (room temperature) and completed in <1 min.

Pupillometry of isolated anterior chamber. An enucleated eye from an overnight-dark-adapted mouse was hemisected just posterior to the limbus. All posterior tissue was removed, leaving the anterior chamber consisting of cornea, iris and supporting tissue. The preparation was maintained in pre-oxygenated L-15 medium at 23^{o}C (room temperature), with 0.5% atropine added to block the activity of any parasympathetic synaptic transmission. Video recording was done under infrared illumination, and Xe light was delivered via a light guide with output positioned at ~1 cm from the preparation.

Iris-sphincter-muscle force measurements. An enucleated eye from an overnight-dark-adapted mouse was used. The iris sphincter muscle encircling the pupil was excised by a circumferential cut at ~200 μm from the pupil perimeter. The muscle ring was transferred into the recording chamber and superfused with Ames medium (equilibrated with 95%O_2/5%CO_2) at 35-37ºC and a flow rate of 2 ml min^{-1}. With infrared light and viewers, the muscle ring was mounted horizontally on an upright microscope between two stainless-steel hooks attached to micromanipulators. Dissection and mounting required ~5 min for the mouse. One hook was fixed and the other attached to a force sensor (see below). The muscle ring was slowly stretched to a length of 1.2-1.6 mm, so that the overall sphincter muscle length (2.4-3.2 mm) was about half of the circumference of the dark-adapted mouse pupil, which by trial and error was found to give roughly maximum force-generation. The iris preparation was stable, giving reproducible light responses for over 6 hours. Similar procedures were used for all other species, with appropriate adjustments for the different sizes of the sphincter muscle from different species. For certain species, it was impossible to dark-adapt the animal overnight before experiments or even dark-adapt at all; in these cases, the eye was hemisected or dissected open immediately upon removal from the animal, and immersed in oxygenated Ames solution in a light-proof box for ~1 hr (including transport). The time duration between death of the animal and setting up of the muscle preparation was, however, mostly < 1 hour for the majority of species.

Muscle force was measured with a fabricated device containing a single-crystal silicon string-gauge with μNewton sensitivity (AE-801, Sensor One), and the signal was amplified with custom circuitry. The force sensor was coated with a suspension of carbon powder in silicone in order to protect it from light and moisture. The voltage output of the sensor was proportional to

the applied force (137 μN/V), with a non-linearity of <0.1% (Fig. S11). The signal was digitized by Digidata 1322A and acquired by pClamp 9.0.

The action spectrum of the light-induced muscle force was determined with dim-flash responses that were linearly proportional to stimulus strength. The sensitivity (i.e., the transient-peak-force/light-intensity ratio) at different wavelengths was normalized to unity at the highest value. Light was delivered through a 5X objective as a uniform spot of 3-mm diameter on the muscle for mouse, large enough to cover the entire preparation. For all other species, the light spot was 5 mm in diameter (maximal opening of the microscope field aperture) on the muscle, large enough to cover the whole sphincter-muscle preparation from rat, hamster, guinea pig, cat, rabbit and other small animal species, but only ~70-90% of the preparation for dog, pig and monkey. None of the flash stimuli in the experiments reported here produced a detectable temperature increase, as measured by a miniature thermistor placed at the same position as the muscle sample with normal bath perfusion at 35-37^{o}C. A monochromatic (436-nm) light step elevated temperature by <0.1^{o}C that reached steady state in 5 s after light was turned on. This temperature change was within the normal temperature fluctuations (±0.2^{o}C) in the bath solution and did not produce spontaneous muscle contractions. For pig and monkey, a step of intense white light did trigger a detectable muscle contraction, but with a rather unusual shape and no sign of adaptation even upon repeated light stimulation. Such a step of intense white light also produced a temperature change of ~1.4^{o}C (reaching steady state in ~5 s after light on). These muscle responses were probably artifacts, and have not been included in this paper.

***In situ* pupillometry.** Head-fixed mice were used for pupillometry in order to enable long-duration measurements[16]. Mice were anesthetized with an intraperitoneal injection of Tribromoethanol (Avertin) (250mg/kg). A patch of skin overlying the skull was excised, and

four bone screws were threaded into the skull, with care taken to prevent any damage to the brain. These screws were covered with dental cement, and served as the foundation for a stainless-steel post. For pupillometry, this post was clamped in order to immobilize the mouse head within an acrylic holder, with both eyes positioned for stimulation and video recording. The operated mice were used for pupillometry in at least 7 days postsurgery.

The mice were kept in 12/12-hour light/dark cycles. All PLR experiments were performed between 2 hours after light-on and 2 hours before light-off with >1-hr dark adaptation. To measure the PLRs in both eyes simultaneously, we built a pupillometer with Xenon (Xe) or LED light for stimulation via a Ganzfeld sphere[15]. The stimulated eye was monitored continuously from inside the Ganzfeld sphere with a miniature, infrared CCD camera (with an 850-nm long-pass filter) and >850-nm infrared light from a LED, both accessing the sphere interior via small holes (2mm and 4 mm in diameter, respectively). The unstimulated eye outside the sphere was monitored with another infrared CCD camera and infrared light. Light in the Ganzfeld interior was prevented from leaking out and stimulating the other eye by the use of foam lining around the stimulated eye. Videos for both eyes were digitized and recorded at a frame rate of 5 Hz. A data-acquisition board (NI USB-6211, National Instruments) and custom software were used for triggering recordings and light stimulation simultaneously. Videos were analyzed at 1 frame/s with custom routines in Image J (Ref. 15). The maximum pupil constriction in the ipsilateral, illuminated eye (i.e., direct PLR) during the 2-min light period was measured (and averaged over a 2- to 10-s time window in that temporal vicinity), and the contralateral pupil (i.e., consensual PLR) was measured over the same time window for comparison. Both pupil area and diameter were provided, the first in keeping with earlier work[10] and the second for its utility because of its potentially linear relation with sphincter-muscle

force[17]. When needed, 5 μl of 600-μM TTX in water was topically applied to the ipsilateral cornea. Pupil measurement was performed in 5 to 45 minutes after TTX administration. The effectiveness of TTX in this time window was confirmed in non-operated *Opn4*$^{-/-}$ mice by the disappearance of all PLR in the TTX-treated eye when light was delivered to the same eye or to the contralateral eye.

For *in situ* PLR measurements in monkey, the setup was somewhat different. Both eyes were illuminated by an infrared (>850nm) light source and videoed simultaneously with an infrared CCD camera coupled to a macro lens. A 505-nm LED or bright-white LED was positioned at ~4 cm from one eye and delivered 3.1×10^{-4} and 9.3×10^{-4} μW μm^{-2} light respectively, at the cornea. Illumination of an eye covered by an opaque corneal protector did not cause any constriction of the contralateral pupil in an unoperated animal, thus ruling out any confounding effect of light scatter. The 505-nm LED was first used. If no PLR was observed, the bright-white LED was used in addition to the 505-nm LED.

Intraorbital optic-nerve transection in mouse. Mice were anaesthetized and fine forceps used to transect the lateral rectus and part of the superior rectus and superior oblique extraocular muscles. This procedure allowed the eye to be gently lifted from the socket with ring forceps, exposing the optic nerve. The dural sheath of the nerve was opened with fine forceps and the nerve transected at a distance of 1-2 mm from the eyeball. As a result, the two cut ends of the optic nerve often retracted and became separated by a distance of >2 mm; in some cases, a few millimeters of the optic nerve was physically removed to ensure full transection. The ocular blood supply was not disturbed. Animals were allowed to recover for >1 week before experimentation. Typically, the optic nerve of only one eye of an animal was transected in order to allow uninterrupted circadian photoentrainment of the mouse and its PLR. When only the eye

with transected optic nerve was illuminated, the non-denervated eye never responded, confirming no signal transmission from the denervated eye to the brain.

Immunocytochemistry of albino-mouse iris. Because the typical mouse iris is heavily pigmented with melanin, we used an albino background (C57BL/6J-Tyr^{c-2J}/J, Jackson Labs) for these experiments. Fresh eyes were pierced near the limbus and fixed for 2 hours at room temperature in 4% paraformaldehyde in PBS. After washes and overnight cryoprotection in 30% sucrose (in PBS) at 4°C, an eye was hemisected just posterior to the limbus. All posterior tissue and lens were removed. The anterior part of the eye, including the iris, was embedded in OCT (Tissue-Tek) and cross-sectioned at 10–20 μm thickness. The sections were mounted on glass slides and blocked with 5% goat serum in 0.3% Triton X-100 in PBS for 1 hour at room temperature. They were then incubated overnight at 4°C in the same blocking solution with a polyclonal antibody against melanopsin (AB-N38, Advanced Targeting Systems) at 1:10,000 dilution and a monoclonal antibody against smooth-muscle α-actin (ab18460, AbCam) at 1:1,000 dilution. After washing, the sections were exposed to secondary antibodies (*Alexa Fluor® 488* goat anti-rabbit IgG and *Alexa Fluor® 633* goat anti-mouse IgG) at 1:1000 dilution for 1-3 hours at room temperature. Sections were mounted with anti-fade reagent containing 4',6'-diamidino-2-phenylindole (DAPI) and coverslipped.

Visualizing fluorescence reporter in freshly-isolated iris. To avoid the melanin pigmentation, an albino background (C57BL/6J-Tyr^{c-2J}/J, Jackson Labs) was also used for this experiment. A freshly isolated anterior chamber with cornea and iris was held down mechanically in Ames solution, with posterior side facing up. Because the red fluorescence of the iris in the *Opn4:tdTomato* BAC transgenic line was extremely weak, the signal was detected by a sensitive silicon-intensified target (SIT) camera (C2400-08, *Hamamatsu*) or an EMCCD

camera (LUCA^{EM}, *Andor*) coupled to an upright Zeiss microscope. An *Opn4:tdTomato* iris was always compared side-by-side with a non-transgenic albino iris serving as a negative control (C57BL/6J-Tyr^{c-2J}/J).

Reverse-transcription polymerase chain reaction (RT-PCR). One or more irises dissected far from, and clear of, the ciliary body were washed 3 times in PBS, homogenized in TRIzol reagent (Invitrogen), and the RNA extracted by phase-separation. The RNA was then treated with RQ1 DNase and reverse-transcribed by the SuperScriptTM III First-Strand Synthesis System (Invitrogen). The resulting cDNA was amplified with specific primer pairs and the PCR products visualized by electrophoresis using 1.5% agarose gels. The PCR reaction used 30 cycles with annealing temperature at 55°C. β-actin served as a positive control and *PNR*, a photoreceptor-specific nuclear receptor protein, was a marker for contamination from retinal tissue. The following PCR primers were used: mouse *Opn4* (*5'-CCC CTG CTC ATC ATC ATC TTC TG-3'* and *5'-TGA CAA TCA GTG CGA CCT TGG C-3')*, mouse *PNR* (*5'-AGA AGG AGT CTC CAG GTA GAT G-3'* and *5'-CTG CTT GTA AGC ACT TCT TCA G-3'*), *mouse β-actin* (*5'-ACA GGA TGC AGA AGG AGA TTA C-3'* and *5'-GTG TAA AAC GCA GCT CAG TAA C-3'*), mouse *Trpc7* (*5'-GAA CTT GCA AGT CTG GTC CGA CC-3'* and *5'-CAG CGT TAC ATC CTG CAC GTA CTG-3'*), mouse *rhodopsin* (*5'-CTA CAC ATC ACT CCA TGG CTA C-3'* and *5'-CAT GTA GAT GAC AAA GGA TTC G-3'*), monkey *Opn4* (*5'-CTT CTG TGG GGC TCT CTT TG-3'* and *5'-GGA GGA AGA ACA CGA AGC AG-3'*), monkey *PNR* (*5'-TAA GCT GGA GCC AGA GGA TG-3'* and *5'- ATC ACT TGG GAC TGG TCC TG-3'*) and monkey *β-actin* (*5'-TCC CTG GAG AAG AGC TAC GA-3'* and *5'-CTT CTG CAT CCT GTC AGC AA-3'*).

Single-cell electrophysiology. A mouse was dark-adapted overnight, anesthetized by Avertin, and enucleated before euthanasia. An eye was hemisected, the retina teased free, and

the vitreous removed with fine forceps. For flat-mount recording, the retina was flattened with cuts and held in the recording chamber, photoreceptor-side down, by a platinum-iridium frame strung with nylon fibers. For dissociated-cell recording, the retina was cut into pieces and exposed for 30 min at 35°C to a protease solution (bicarbonate-buffered "ionic Ames," indicated below, containing 0.25 mg/ml Protease XXIII (Sigma-Aldrich) and 50 U/ml collagenase IV (Worthington). The pieces were rinsed with ionic Ames, transferred to the same solution containing 1 mg/ml BSA and 1 mg/ml trypsin inhibitor at room temperature, and kept until use over a period of 8 hours. As needed, several pieces were transferred into a dissociation solution (see below) and triturated to give dissociated cells.

All recordings were in the perforated-patch, voltage-clamp mode at V_{hold} = -80 mV, with junction potential corrected and series resistance monitored. Carried out on a Zeiss upright microscope, some recordings were at room temperature, ~23 °C (for stability). Recordings were also made at 35^{o}C by warming the bath solution (Ames medium) with an inline heater (Warner Instruments, Hamden, CT). Solution ran at ~5 ml/min through the 1-ml experimental chamber. Temperature was monitored by a thermistor in the chamber. IpRGCs were identified by their expression of tdTomato under the control of the melanopsin BAC transgene[15]. TdTomato was visualized with standard filter sets for Cy3 fluorescence. To minimize photobleaching of the cells, we used relatively dim epi-fluorescence excitation flashes, which picked up only ipRGCs with the brightest tdTomato signals. After cell identification, the optics was switched to infrared-DIC microscopy. For the flat-mount retina, the inner limiting membrane overlying the ipRGC was removed with an empty patch-pipette prior to recording. The infrared field-illumination was greatly attenuated or turned off during electrical recording, except for viewing during intermittent corrections of the cell or pipette position. The Faraday cage itself was light-

proof. The ipRGCs identified in the above manner should be of the M1-subtype, which in WT and certain KO genotypes could be readily validated by their much higher photosensitivity and very much larger photocurrents compared to the other ipRGC subtypes.

In experiments carried out at 35°C, we also took the extra step of labeling the recorded ipRGCs afterwards with an intracellular dye (100-μM Alexa Fluor 555) dialyzed from a separate whole-cell patch pipette. Such labeling confirmed that the recorded cells were all M1-ipRGCs, based on the projection of their dendritic arborizations to the off-sublamina of the inner plexiform layer.

Data acquisition proceeded on two channels. The first was low-pass filtered at 10 kHz (Bessel) and sampled at 50 kHz, in order to resolve a capacity transient (and leak current) induced with each sweep to monitor the series resistance, input resistance, and cell capacitance. The second was filtered at 10 Hz and sampled at 40 Hz, in order to resolve the photocurrent. Data were analyzed with custom routines written in Igor 3.14 (Wavemetrics) or Origin (Origin Lab Corp.) and presented as mean ± S.E.M.

Solutions. For perforated-patch recordings, the unsupplemented pipette solution contained (in mM): 110 KCl, 13 NaCl, 2 $MgCl_2$, 1 $CaCl_2$, 10 EGTA, 10 HEPES, 0.125 Amphotericin B, pH 7.2 with KOH. This intracellular solution was KCl-based. Many other anions have been tested, but Cl^- gave the lowest and most stable series resistances, especially in combination with the chosen EGTA concentration. Amphotericin B was dissolved in DMSO to make 100X aliquots, and stored in the dark at -20° C for up to two weeks. Amphotericin-containing internal solution was sonicated before loading into each patch-pipette. The bath solution was Ames medium. For recordings from the flat-mount retina, fast synaptic transmission was blocked by adding 3-mM kynurenate, 100-μM picrotoxin and 1-μM strychnine to the bath solution. On rare

occasions, some synaptic transmission persisted in this cocktail (evidenced by a short-latency, transient light response preceding the intrinsic light response) and was abolished by adding 100-µM D,L-AP4. Sometimes, kynurenate was replaced by 50-µM D,L-AP5, 20-µM DNQX (or CNQX) and 100-µM hexamethonium bromide. A liquid-junction potential of +3 mV has been corrected.

The protease solution for retinal dissociation consisted of bicarbonate-buffered ionic Ames with enzymes (see above). This ionic Ames was formulated with ion concentrations similar to those in Ames but without other supplements: (in mM) 120 NaCl, 22.6 $NaHCO_3$, 3.1 KCl, 0.5 KH_2PO_4, 1.5 $CaCl_2$, 1.2 $MgSO_4$, 6 glucose, equilibrated with 95% O_2/5% CO_2. The "dissociation solution" for trituration had (in mM): 70 Na_2SO_4, 2 K_2SO_4, 5 $MgSO_4$, 10 HEPES, 10 glucose, 60 sucrose, pH 7.4 with NaOH. 0.05% DNase (Worthington) was sometimes added to reduce cell clumping following trituration.

In iris sphincter-muscle force measurements, acetylcholine or 0-Ca^{2+} bath solution was applied by switching the bath perfusate to the respective solution. In the 0-Ca^{2+} experiment, the control bath solution was ionic Ames and the 0-Ca^{2+} solution contained 1-mM EGTA and 2.7 mM $MgCl_2$. For some force measurements on the rhesus-monkey iris-sphincter muscle, Ames with 30-µM 9-*cis*-retinal (a readily available homolog of 11-*cis*-retinal) in 0.1% ethanol at 35-37°C was admitted into the recording chamber for up to an hour before light stimulation.

X-gal labelling. The isolated retina or the anterior chamber with iris was fixed for 10 minutes at 4°C in PBS (pH 7.4) containing 0.2% glutaraldehyde, 0.5-mM EGTA and 2-mM $MgCl_2$, then washed 3 times each for 5 min in washing buffer (2-mM $MgCl_2$, 0.01% Na-desoxycholate, and 0.02% NP40 in PBS pH 7.4). The samples were then incubated overnight in

the staining solution (washing buffer plus 5-mM K-ferricyanide, 5-mM K-ferrocyanide, and 1-mg/ml X-gal). The samples were then kept overnight in washing buffer at 4°C to intensify the signal. Blue X-gal staining was checked under a microscope.

Immunoprecipitation. For immunoprecipitation (IP), retinal proteins were isolated from a 4-week-old mouse and solubilized in IP buffer containing 20-mM HEPES–NaOH (pH 7.5), 1% Triton X-100, 150-mM NaCl, and a protease inhibitor cocktail. One milligram of soluble proteins was used for IP with 5-µg of the antibody and 10-µg protein A sepharose (Amersham Pharmacia Biotech). For western blotting, a concentration of 5 mg/ml of a polyclonal antibody against TRPC7 (epitope sequence CKDHRVNQGKD) was used. A 1:10,000-diluted secondary goat anti-rabbit IgG conjugated with HRP (Pierce Biotechnology, Rockford, IL) was applied to the blot for 1 hour at room temperature. The signals were visualized on X-ray film using an ECL kit from Pierce Biotechnology.

Light stimulation. A 75-watt Xe-arc lamp, with light passing through a heat filter, calibrated neutral-density filters, 10-nm bandpass interference filters and an electronic shutter, was used in experiments on the isolated eye, isolated anterior chamber, some *in vivo* pupillometry, and some ipRGC electrophysiology. A 100-watt Hg-arc lamp, with light transmitted through a similar path, was used in the iris-muscle-force measurements. An LED light source was used for some of the *in vivo* pupillometry and ipRGC electrophysiology experiments. Hg light was used in conjunction with an interference filter, most often centered at 436-nm (10-nm bandwidth) in order to admit the Hg line closest to the λ_{max} of melanopsin (480 nm). LED light was produced by a "super-bright" LED (λ_{max} at 505 nm, with 30-nm bandwidth) with controlled intensity and duration via custom circuitry, and passed through a pinhole to

produce dimmer light in some *in vivo* PLR experiments. Light intensities were regularly calibrated with a radiometer.

To stimulate ipRGCs *in vitro,* light was delivered through a light guide into the epifluorescence port of the microscope. To stimulate the iris muscle *in vitro,* light was delivered directly to the microscope. Within the microscope, all light was passed through a field aperture for control of the spot size, reflected off a cold mirror to minimize heat, and focused onto the preparation through a 40X or 5X objective, to give a light spot of 730 μm or 5 mm in diameter. The 730-μm light spot was for stimulating ipRGCs and was sufficient for covering uniformly the entire dendritic arbor of a cell in the flat-mount retina. The 5-mm light spot was for stimulating the iris muscle, and was sometimes reduced to 3 mm by a diaphragm for smaller muscles.

To stimulate the isolated eye or anterior chamber *in vitro*, light was brought directly to the preparation through a light guide. To trigger the PLR *in vivo*, an LED was mounted directly on the Ganzfeld diffusing sphere. In order to stimulate with the equivalent of room light or sunlight, this LED was replaced by a light guide coupled to a Xe-arc light source with an additional 400-650 nm bandpass filter. The Ganzfeld produced adirectional light at the cornea. Sufficient time was allowed between stimuli in order for the cell, tissue, or animal to completely recover.

To facilitate comparisons, in all experiments involving melanopsin-mediated photoresponses, the light regardless of source was also converted to "equivalent" 480-nm monochromatic light for data analysis and display, by using the normalized action spectrum of melanopsin, $f(\lambda)$, and the power-scaled spectrum of the light stimulus, $L(\lambda)$. The conversion ratio is:

$Power_{equivalent\ 480nm\ light} = Power\ ratio \times Power_{light\ with\ L(\lambda)\ spectrum}$, where

$$Power\ ratio = \frac{\frac{hc}{480}\int\left(\frac{L(\lambda)}{hc/\lambda}\times f(\lambda)\right)d\lambda}{\int L(\lambda)\,d\lambda} = \frac{\int(\lambda\times L(\lambda)\times f(\lambda))\,d\lambda}{480\int L(\lambda)\,d\lambda}$$

The spectra of the LED and the Xe-arc lamp were provided by the manufacturers. Light from an arc lamp (Hg or Xe), when used with interference filters, could be converted directly to equivalent 480-nm light based on the melanopsin action spectrum. When white arc light was used on ipRGCs and iris muscles for saturating the response, the white flashes were converted to equivalent 480-nm flashes by response-matching in the linear range with dim light. For sunlight, standard tables from ASTM (G173-03 Standard Tables for Reference Solar Spectral Irradiances, http:// rredc.nrel.gov/solar/spectra/am1.5/#about) were used. Ambient sunlight intensity was measured on a clear day in Baltimore, MD at noon, with the radiometer oriented parallel to the ground for measuring ambient light (~4×10^{-5} μW μm^{-2}) and toward the sun to measure direct sunlight (~4×10^{-4} μW μm^{-2}). Room-light intensity was measured at several locations in the room, at the level of a laboratory bench (~1×10^{-6} to ~4×10^{-6} μW μm^{-2}). In order to compare only within the visible-light spectral range, a 400-650 nm bandpass filter was used in front of the radiometer for both sunlight and room-light measurements. Because room light has complex and variable spectra, we simply assumed its spectrum to be the same as the sunlight spectrum. Correspondingly, for simulating room light and sunlight, the Xe white light was filtered by the same 400-650 nm bandpass filter. The Xe light was used to simulate sunlight and room light because it has the closest spectral profile to sunlight than other light sources.

Multiple-linear regression. Multiple-linear regression was performed by a fit function in Origin (Origin Lab Corp.). The ipRGC photocurrent waveforms for *Trpc6*$^{-/-}$ ($f_{Trpc6^{-/-}}$) and

Trpc7$^{-/-}$ ($f_{Trpc7^{-/-}}$) are treated as independent variables, and that for WT (f_{WT}) treated as the dependent variable. The model is of the form:

$$f_{WT} = \beta 1 \times f_{Trpc6^{-/-}} + \beta 2 \times f_{Trpc7^{-/-}} + \varepsilon$$

where ß1, ß2 are the coefficients and ε is the error term. The error term represents the unexpected or unexplained variation in the dependent variable. We assume that the mean of the random variable ε is zero. Parameters are estimated by a weighted least-squares method. Entire 60-sec light-response waveforms were used for the regression. However, only the first 30 sec of data are plotted in Fig. S6 to focus on the rising and falling phases of the response.

***In situ* monkey PLR experiments.** A rhesus monkey (*Macaca mulatta*, 2 animals used altogether) was sedated with ketamine (20 mg kg^{-1}, intramuscular), then anesthetized with either sodium pentobarbital (25 mg kg^{-1}, intravenous, followed by constant infusion at 10 mg kg^{-1} hr^{-1}) or the gas anesthetic, isoflurane (0.5-2%). The animal was placed on a heating pad, and the vital signs were monitored (body temperature, heart rate, and respiration). Both eyes were fitted with opaque contact lenses/corneal protectors to promote dark adaptation and all subsequent steps were performed under dim red light.

For the first animal, after the lateral orbital wall was removed, the left optic nerve was transected, upon which the pupil immediately dilated from a highly constricted state (the oculomotor nerve, which runs separately in primate, was spared). Care was taken to transect the optic nerve at least 5-6 mm posterior to the insertion into the globe to avoid severing the central retinal artery. The right optic nerve (but again not the oculomotor nerve) was transected using a medial approach that required minimal manipulation of the bone. Again, obvious dilation of the pupil was observed without any compromise to the retinal circulation. Pupillometry was then

performed as described above. No direct response to light was seen in either eye, but pentobarbital prevented the use of the consensual pupillary response as a positive control by immobilizing the pupils.

For the second animal, only the right optic nerve was transected from the medial side. By adjusting the isoflurane to a level just sufficient for maintaining anesthesia (see below), the consensual PLR was preserved.

In both animals, indirect ophthalmoscopy confirmed continuous blood flow to the retina after optic-nerve transaction.

The same was carried out for the owl monkeys (see below).

SUPPLEMENTARY TEXT

***In situ* rhesus-monkey PLR**. For one animal, which was under pentobarbital anesthesia, bright illumination (with an indirect ophthalmoscope) prior to optic-nerve transection failed to produce either a direct or consensual PLR in either eye. Under similar scotopic conditions in the absence of anesthesia, the pupils were normally reactive. Thus, we attributed the lack of PLR to the effects of pentobarbital and any residual ketamine. Transection of the optic nerves in both eyes led to immediate dilation of the pupils, suggesting the release of some tonic activation of the iris sphincters or inadvertent damage to the pupillomotor fibers in the oculomotor nerve. The baseline absence of any PLR made the determination of an afferent versus efferent effect impossible. Prolonged direct illumination of either eye failed to produce any pupillary constriction, consistent with the absence of an intrinsic PLR. However, this finding was inconclusive due to the lack of pupillary movements even before optic-nerve transection.

For another animal, which was under titratable isoflurane anesthesia (0.5-2%), bright illumination of either eye prior to surgery produced an obvious constriction of both pupils (direct

and consensual PLRs). Illumination of an eye covered with the opaque corneal protector did not cause any constriction of the contralateral pupil, ruling out any confounding effect of light scatter. After transection of the right optic nerve, even prolonged illumination of the right eye failed to produce any constriction of the right pupil, indicating no intrinsic PLR. Moreover, illumination of the right eye did not elicit a reaction in the left eye, confirming the presence of a complete optic-nerve transection. However, illumination of the unoperated left eye did produce constriction of both pupils, demonstrating that the function of the iris sphincter in the operated right eye was normal. Together, these data suggest that the rhesus monkey has no intrinsic PLR.

***In situ* owl-monkey PLR**. Two animals (*Aotus azarae*) were used, with titratable isoflurane anesthesia (0.5-4%). Similar procedures were followed as for the second rhesus monkey. Bright illumination after optic-nerve transection failed to produce any direct PLR in the operated eye, although infraorbital injection of ~0.1 ml 1-mM carbachol into the anterior chamber triggered a robust PLR in the operated eye, suggesting normal sphincter-muscle function. These data suggest that the owl monkey has no intrinsic PLR.

Human patients. During our routine clinical care, we encounter patients with unilateral optic neuropathies resulting in the complete absence of light perception (glaucoma, D.S.W.; trauma, S.L.M.). In these patients, illumination of the unaffected eye produces constriction of both pupils, but when the light source is quickly moved to the affected eye, both pupils dilate to their steady-state size. If the order is reversed, illumination of the affected eye produces no constriction in either eye. These observations are consistent with the primate data and suggest the absence of an intrinsic PLR in humans.

References

1. Freichel, M., Suh, S.H., Pfeifer, A., Schweig, U., Trost, C., Weissgerber, P., Biel, M., Philipp, S., Freise, D., Droogmans, G., Hofmann, F., Flockerzi, V. & Nilius, B. Lack of an endothelial store-operated Ca2+ current impairs agonist-dependent vasorelaxation in TRP4-/- mice. *Nat Cell Biol* **3,** 121-127 (2001).

2. Weissgerber, P., Held, B., Bloch, W., Kaestner, L., Chien, K.R., Fleischmann, B.K., Lipp, P., Flockerzi, V. & Freichel, M. Reduced cardiac L-type Ca2+ current in Ca(V)beta2-/- embryos impairs cardiac development and contraction with secondary defects in vascular maturation. *Circ Res* **99,** 749-757 (2006).

3. Farley, F.W., Soriano, P., Steffen, L.S. & Dymecki, S.M. Widespread recombinase expression using FLPeR (flipper) mice. *Genesis* **28,** 106-110 (2000).

4. Schwenk, F., Baron, U. & Rajewsky, K. A cre-transgenic mouse strain for the ubiquitous deletion of loxP-flanked gene segments including deletion in germ cells. *Nucleic Acids Res* **23,** 5080-5081 (1995).

5. Jiang, H., Lyubarsky, A., Dodd, R., Vardi, N., Pugh, E., Baylor, D., Simon, M.I. & Wu, D. Phospholipase C beta 4 is involved in modulating the visual response in mice. *Proc Natl Acad Sci U S A* **93,** 14598-14601 (1996).

6. Dietrich, A., Kalwa, H., Storch, U., Mederos y Schnitzler, M., Salanova, B., Pinkenburg, O., Dubrovska, G., Essin, K., Gollasch, M., Birnbaumer, L. & Gudermann, T. Pressure-induced and store-operated cation influx in vascular smooth muscle cells is independent of TRPC1. *Pflugers Arch* **455,** 465-477 (2007).

7. Hartmann, J., Dragicevic, E., Adelsberger, H., Henning, H.A., Sumser, M., Abramowitz, J., Blum, R., Dietrich, A., Freichel, M., Flockerzi, V., Birnbaumer, L. & Konnerth, A. TRPC3 channels are required for synaptic transmission and motor coordination. *Neuron* **59,** 392-398 (2008).

8. Dietrich, A., Mederos, Y.S.M., Gollasch, M., Gross, V., Storch, U., Dubrovska, G., Obst, M., Yildirim, E., Salanova, B., Kalwa, H., Essin, K., Pinkenburg, O., Luft, F.C., Gudermann, T. & Birnbaumer, L. Increased vascular smooth muscle contractility in TRPC6-/- mice. *Mol Cell Biol* **25,** 6980-6989 (2005).

9. Suzuki, M., Mizuno, A., Kodaira, K. & Imai, M. Impaired pressure sensation in mice lacking TRPV4. *J Biol Chem* **278,** 22664-22668 (2003).

10. Lucas, R.J., Hattar, S., Takao, M., Berson, D.M., Foster, R.G. & Yau, K.-W. Diminished pupillary light reflex at high irradiances in melanopsin-knockout mice. *Science* **299,** 245-247 (2003).

11. Vitaterna, M.H., Selby, C.P., Todo, T., Niwa, H., Thompson, C., Fruechte, E.M., Hitomi, K., Thresher, R.J., Ishikawa, T., Miyazaki, J., Takahashi, J.S. & Sancar, A. Differential regulation of mammalian period genes and circadian rhythmicity by cryptochromes 1 and 2. *Proc Natl Acad Sci U S A* **96,** 12114-12119 (1999).

12. Lem, J., Krasnoperova, N.V., Calvert, P.D., Kosaras, B., Cameron, D.A., Nicolo, M., Makino, C.L. & Sidman, R.L. Morphological, physiological, and biochemical changes in rhodopsin knockout mice. *Proc Natl Acad Sci U S A* **96,** 736-741 (1999).

13. Calvert, P.D., Krasnoperova, N.V., Lyubarsky, A.L., Isayama, T., Nicolo, M., Kosaras, B., Wong, G., Gannon, K.S., Margolskee, R.F., Sidman, R.L., Pugh, E.N., Jr., Makino, C.L. & Lem, J. Phototransduction in transgenic mice after targeted deletion of the rod transducin alpha -subunit. *Proc Natl Acad Sci U S A* **97,** 13913-13918 (2000).

14. Soucy, E., Wang, Y., Nirenberg, S., Nathans, J. & Meister, M. A novel signaling pathway from rod photoreceptors to ganglion cells in mammalian retina. *Neuron* **21,** 481-493 (1998).

15. Do, M.T.H., Kang, S.H., Xue, T., Zhong, H., Liao, H.W., Bergles, D.E. & Yau, K.-W. Photon capture and signalling by melanopsin retinal ganglion cells. *Nature* **457,** 281-287 (2009).

16. Cahill, H. & Nathans, J. The optokinetic reflex as a tool for quantitative analyses of nervous system function in mice: application to genetic and drug-induced variation. *PLoS ONE* **3,** e2055 (2008).

17. Mapstone, R. Forces determining pupil size. *Expl Eye Res* **10,** 47-52 (1970).

18. Govardovskii, V.I., Fyhrquist, N., Reuter, T., Kuzmin, D.G. & Donner, K. In search of the visual pigment template. *Vis Neurosci* **17,** 509-528 (2000).

Supplementary Figure S1

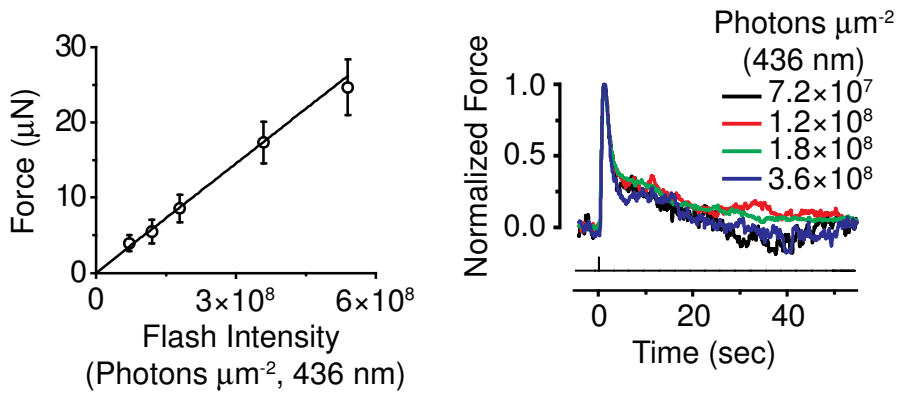

Figure S1. Force responses of mouse iris-sphincter muscle to dim flashes**.** *Left***,** Flash intensity-response relation at transient peak of response (mean ± SEM, 7 muscles). Same data as the foot of the averaged intensity-response relation in Text Fig. 1c, but plotted on a linear flash-intensity axis to indicate linearity. 35-37°C. *Right,* Responses to different dim-flash strengths from the muscle in Text Figure 1c inset, normalized to indicate constant waveform.

Supplementary Figure S2

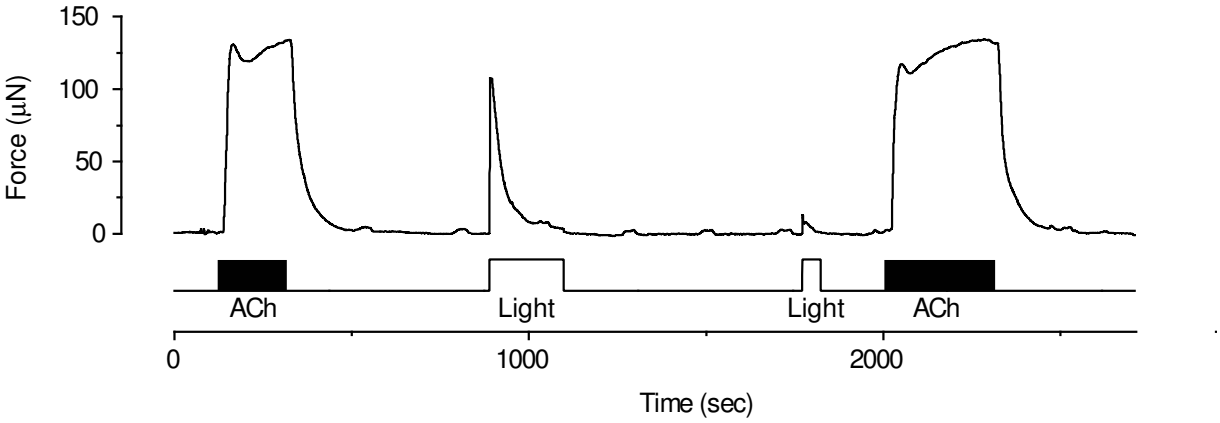

Figure S2. Adaptation of mouse iris-sphincter muscle to a light step, but hardly to acetylcholine steps. Light intensity was 6.1 $\times 10^9$ photons μm^{-2} s^{-1}, 436 nm. The light response declined rapidly despite sustained illumination, and a second light stimulus of the same intensity hardly elicited any response even after 10 minutes in darkness. In contrast, 50-µM acetylcholine applied in bath perfusion elicited a sustained a response, even during adaptation of the muscle to the light stimulus (see also main text). The periodic, small oscillations were presumably spontaneous contractions.

Supplementary Figure S3

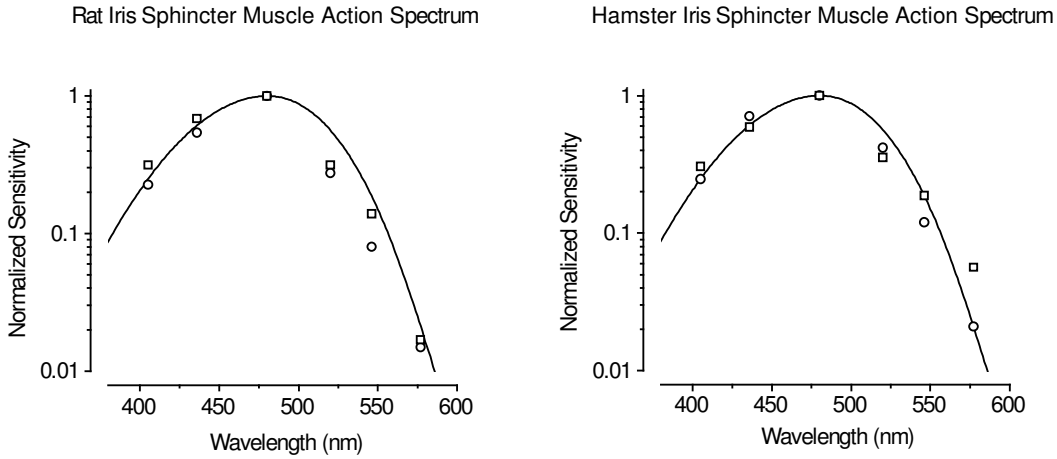

Figure S3. Action spectra of isolated iris sphincter muscle from albino rat and pigmented hamster. Sensitivity normalized to that at 480 nm within each preparation. Two muscles (circle and square) for each kind of animal. Curve in each case is an A_1-pigment spectral template[18] with the λ_{max} of mouse melanopsin (OPN4), 480 nm.

Supplementary Figure S4

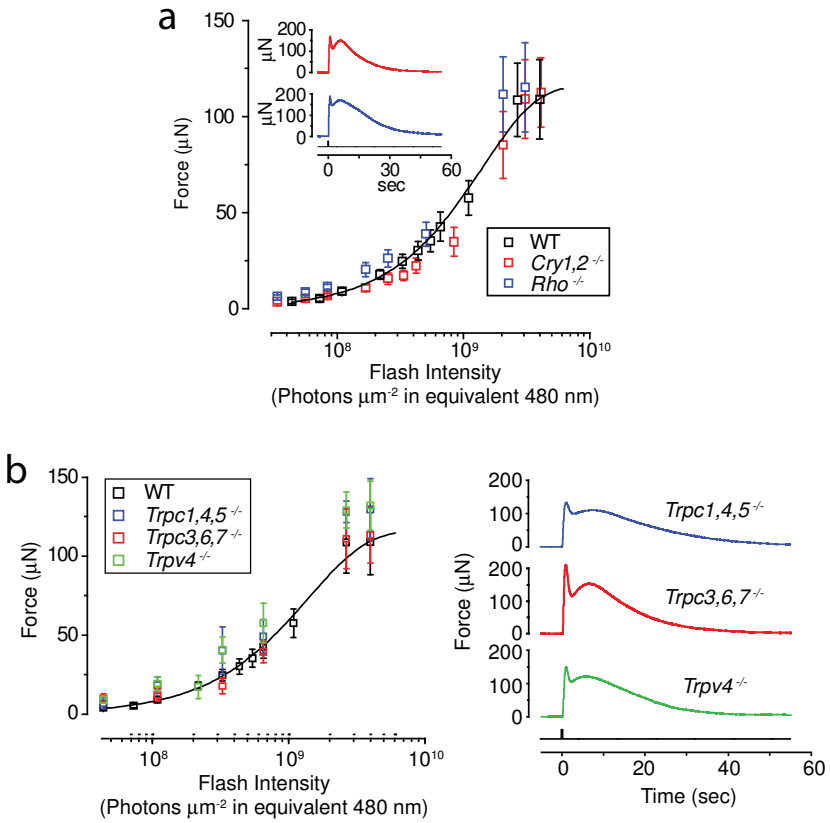

Figure S4. Cryptochromes, rhodopsin and the TRPC channels tested apparently are not involved in intrinsic PLR. **a**, Average flash intensity-response relations for *Cry1,2*$^{-/-}$ (4 muscles) and *Rho*$^{-/-}$ (4) genotypes. WT relation from Text Fig. 1c shown for comparison. *Inset* shows sample responses of *Cry1,2*$^{-/-}$ and *Rho*$^{-/-}$ muscles to a saturating flash of 4.0×10^{9} photons μm^{-2} (equivalent 480 nm). **b,** *Left,* Average flash intensity-response relations for *Trpc1,4,5*$^{-/-}$ (4 muscles), *Trpc3,6,7*$^{-/-}$ (7) and *Trpv4*$^{-/-}$ (4) genotypes. WT relation from Text Fig. 1c also shown for comparison. *Right*, Sample saturated response from each genotype to 4.0×10^{9} photons μm^{-2}. White Hg light for two brightest flashes in intensity-response relations of **a** and **b**, and for all flashes in **b**, right; all other stimuli were 436-nm Hg light. All intensities expressed in equivalent 480 nm photons. Flashes delivered at time 0, as a 3-mm diameter spot covering entire muscle. 35-37°C.

Supplementary Figure S5

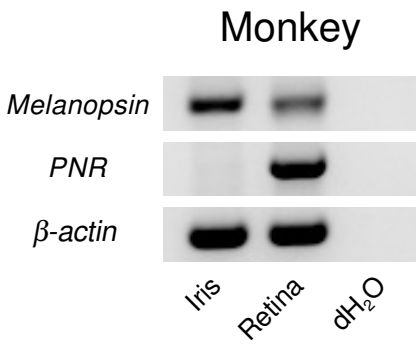

Figure S5. Melanopsin (*Opn4*) mRNA detected by RT-PCR from monkey (baboon; same for rhesus monkey) iris and retina. *PNR* (photoreceptor-specific nuclear receptor) mRNA used as control to rule out contamination from retina to iris. *β-actin* mRNA is a positive control. Difference in melanopsin mRNA signal between iris and retina presumably reflects different fractional total-tissue mRNA coding for melanopsin.

Supplementary Figure S6

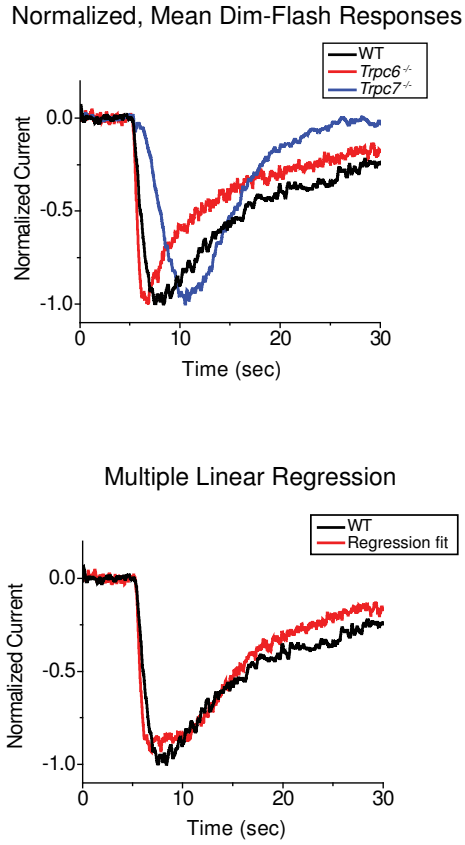

Figure S6. TRPC6 and TRPC7 may not form separate homomeric channels in ipRGCs. *Top*, Averaged dim-flash responses of ipRGCs from WT (6 cells), *Trpc6*$^{-/-}$ (5 cells) and *Trpc7*$^{-/-}$ (5 cells) genotypes normalized and overlaid. *Bottom*, Best fit of WT dim-flash response by combining those of *Trpc6*$^{-/-}$ and *Trpc7*$^{-/-}$ responses based on multiple-linear regression (Methods). The fit is not perfect, thus arguing against separate homomeric channels.

Supplementary Figure S7

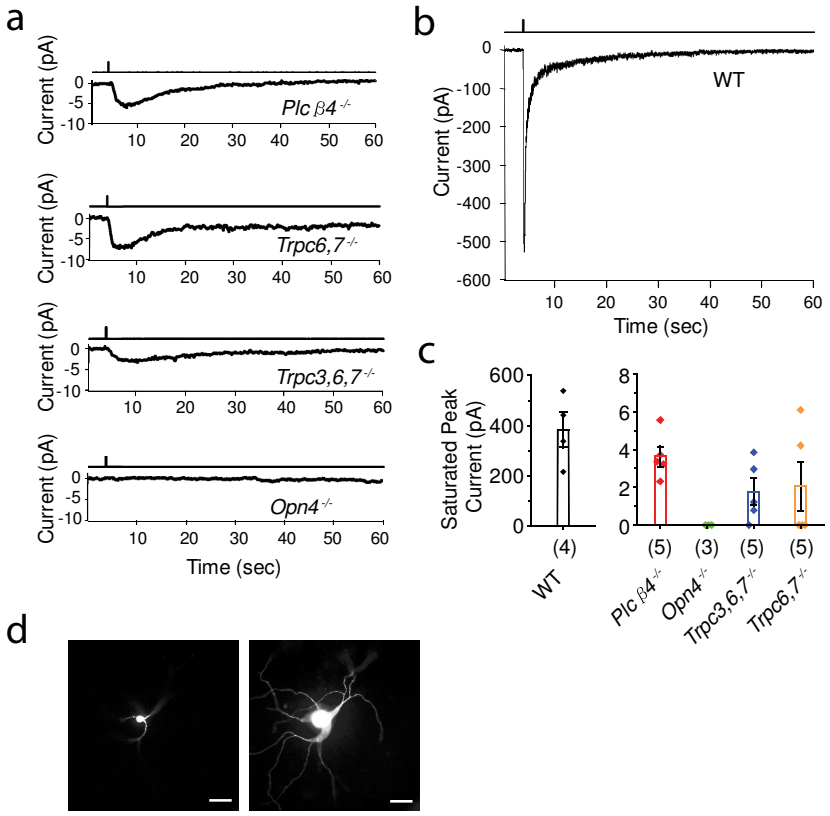

Figure S7. Light responses of M1-ipRGCs of different genotypes at 35°C. **(a)** Examples of saturated flash responses in flat-mount retina from *Plcβ4*$^{-/-}$, *Trpc6,7*$^{-/-}$, *Trpc3,6,7*$^{-/-}$ and *Opn4*$^{-/-}$ M1-ipRGCs. **(b)** Much larger response from WT M1-ipRGC. In all cases, light stimulations were 50-ms, bright-white Xe flashes delivering the equivalent of 1.12 – 1.94 x 10^9 photons μm^{-2} (480 nm). 730-µm-diameter light spot centered on the soma, sufficient to cover the entire intact cell in retina. Light monitor above each trace. All recordings were in perforated-patch, voltage-clamp mode with V_{hold} at -80 mV. Synaptic transmission blocked pharmacologically (see Methods). **(c)** Collective data, with cell numbers of each genotype in parentheses. **(d)** Representative top-view images of a M1-ipRGC with intracellular dye-labeling (Alexa Fluor 555) in flat-mount retina after recording. *Left*, Image with plane of focus at ganglion cell layer, showing cell body and proximal part of dendrites before they dived into the inner plexiform layer. *Right*, Image with plane of focus near the border between inner plexiform layer and inner nuclear layer, showing the dendritic arbors in the off-sublamina of the inner plexiform layer. The soma is out of focus on this plane. Scale bars: 50 µm.

Supplementary Figure S8

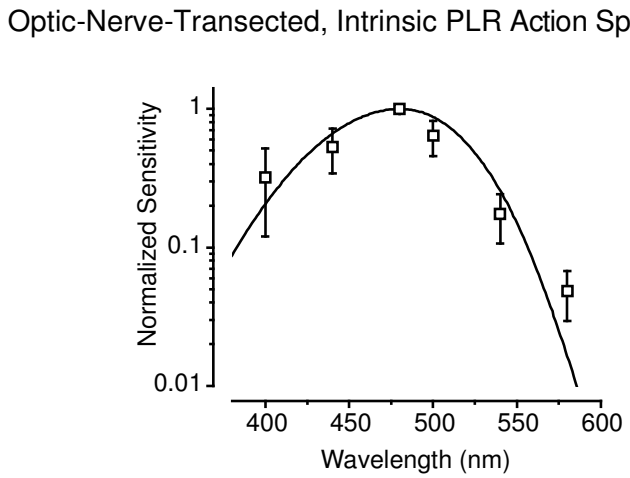

Figure S8. *In situ* ipsilateral-PLR action spectrum for WT mouse with optic nerve transected. Mean ± SEM from 4 animals. Sensitivity defined as fractional pupil constriction at the end of 60-sec illumination (10-nm-bandwidth monochromatic light) divided by photon density, and normalized to that at 480 nm. Curve is an A_1-pigment template[18] with λ_{max} of mouse melanopsin (OPN4), 480 nm. Relatively dim light was used throughout in order to keep the fractional pupil constriction at <35% for all wavelengths.

Supplementary Figure S9

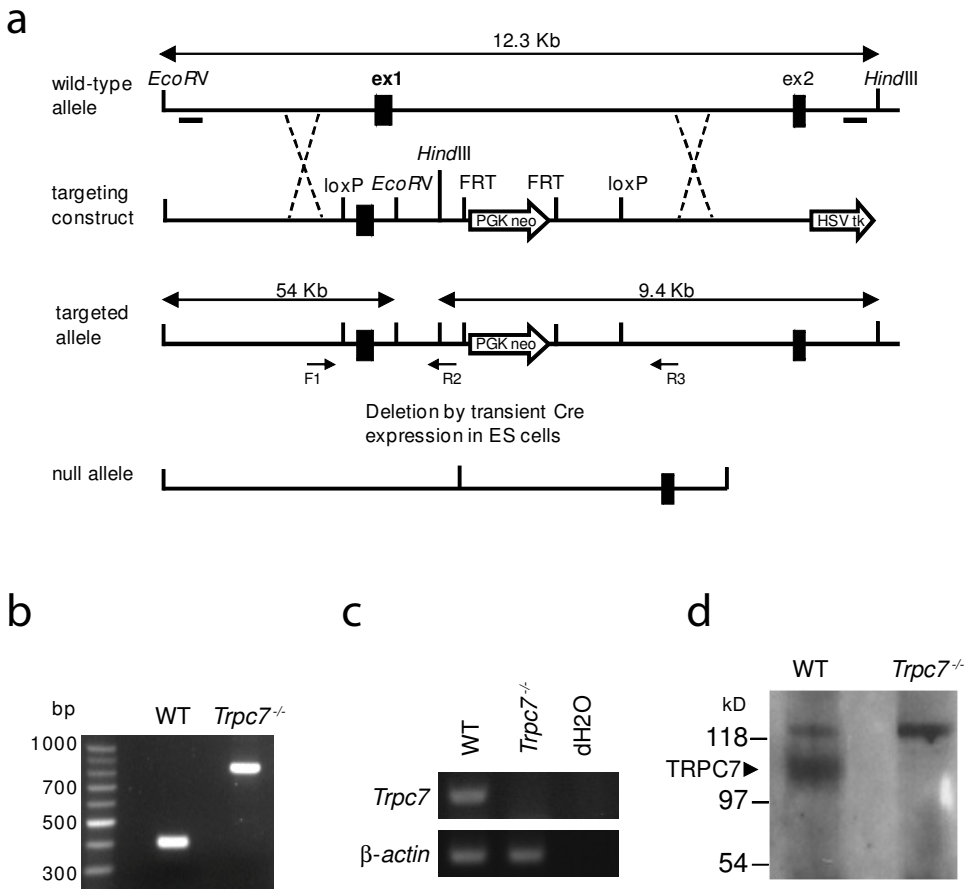

Figure S9. Generation and verification of *Trpc7*$^{-/-}$ mouse. (**a**) Targeting strategy for the disruption of the *Trpc7* gene. Following homologous recombination, the deletion of the exon 1 region was catalyzed by Cre-recombinase in ES cells. (**b**) PCR analysis of tail genomic DNA confirms disruption of the *Trpc7* locus. (**c**) RT-PCR of mRNA extracted from WT and *Trpc7*$^{-/-}$ retinas indicated the absence of Trpc7 mRNA in knockout mouse retina. RT-PCR primers detecting region of exons 2-3 of *Trpc7*. β-actin is the control. (**d**) Immunoprecipitation analysis of TRPC7 protein in retinas extracted from WT and *Trpc7*$^{-/-}$ mice revealed loss of TRPC7 protein in *Trpc7*$^{-/-}$ mice. The arrow (black) indicates the expected position for TRPC7 protein. The bands over 118 kD on both lands are nonspecific.

Supplementary Figure S10

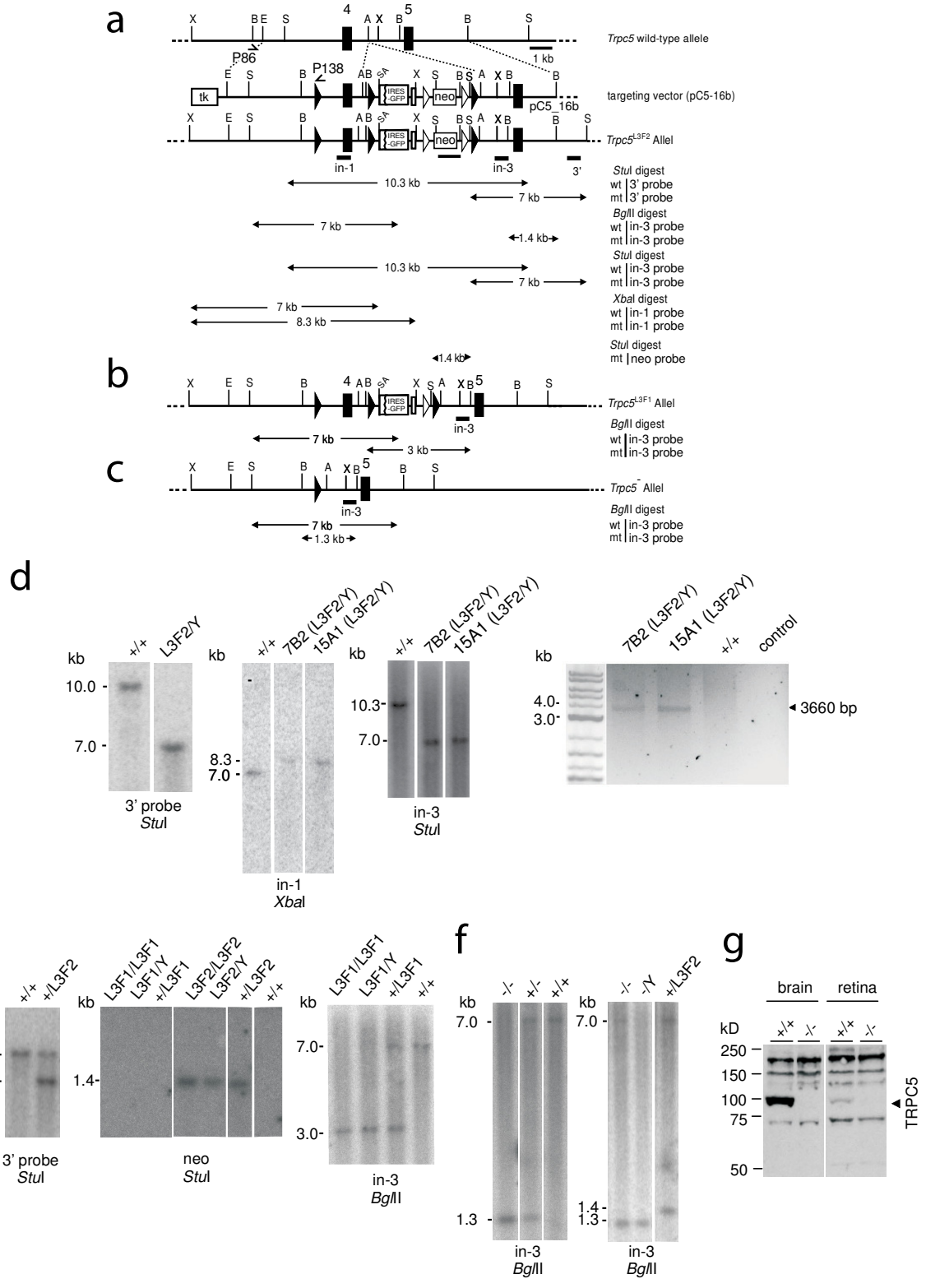

Figure S10. Generation and verification of *Trpc5*$^{-/-}$ mouse. (**a**) Translated exons (not in scale) are shown as filled boxes. Wild-type *Trpc5* allele, targeting construct (pC5-16b) and recombinant *Trpc5*^{L3F2} allele are shown. In the *Trpc5*^{L3F2} allele, exon 4 is flanked by loxP sites (filled triangles) and followed by a splice acceptor (SA)-IRES-GFP cassette, a FRT (open triangles) sequence-flanked pgk-promotor driven neomycin resistance gene cassette (neo^{r}), a third loxP site and the 3‘ homology containing exon 5. X, *Xba*I; E, *EcoR*V; A, *Afl*II; B, *Bgl*II; S, *Stu*I. Probes and sizes of genomic DNA fragments as expected by Southern blots are indicated. (**b**) Flp-mediated conversion of the *Trpc5*^{L3F2} allele to the *Trpc5*^{L3F1} allele. (**c**) Cre-mediated conversion of the *Trpc5*^{L3F2} allele to the *Trpc5*$^{-}$ (*Trpc5*^{L1}) allele. (**d**) Identification of the recombinant *Trpc5*^{L3F2} allele in ES cells by Southern blot analysis using a 3’ probe placed external to the targeted sequence (left panel), internal probes “in-1” and “in-3” (middle panels) indicating singular integration of the targeting vector and amplification of a genomic DNA fragment specific for the *Trpc5*^{L3F2} allele (right panel, arrowhead) using primer P86 located 5‘ of the 5’ homology and primer P138 consisting of sequences of the loxP site to demonstrate correct targeting of the 5’ homologous arm. 7B2 and 15A1 are the two selected ES cell clones. *Trpc5* allele is on X-chromosome. “Y” stands for Y-chromosome. (**e**) Flp-mediated conversion of the *Trpc5*^{L3F2} allele to the *Trpc5*^{L3F1} allele in mice. The *Trpc5*^{L3F2} allele was identified in mice using the 3’ probe (left panel). Mice carrying the *Trpc5*^{L3F1} allele are identified by excision of the PGK-neo^{r} cassette, which generates a 1.4 kb fragment the *Trpc5*^{L3F2} allele detected by the neo probe, and by detection of a 3.0 kb fragment using the “in-3” probe (middle panels). (**f**) Cre-mediated conversion of the *Trpc5*^{L3F2} allele to the *Trpc5*$^{-}$ allele in mice. Mice carrying the *Trpc5*$^{-}$ allele are identified by detection of a 1.3 kb fragment using the “in-3” probe (right panel). (**g**) Immunoblot analysis of TRPC5 protein expression in microsomal membrane protein fractions from brain (left, 150 µg/lane) and lysates from retina (right, 150 µg/lane) extracted from WT and *Trpc5*$^{-/-}$ mice revealed loss of TRPC5 protein in *Trpc5*$^{-/-}$ mice. The arrowhead (black) indicates the expected position for TRPC5 protein. For western blotting, the polyclonal antibody against TRPC5 (epitope sequence KWGDGQEEQV) was diluted 1:2000.

Supplementary Figure S11

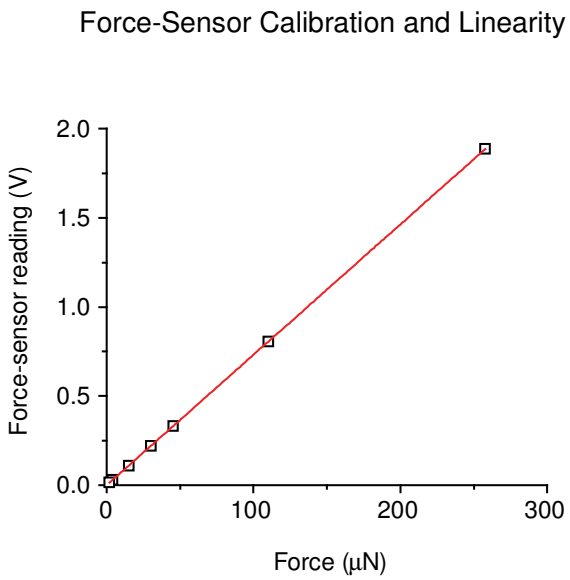

Figure S11. Force-sensor calibration and linearity. The force sensor was calibrated by hanging various pre-measured weights fabricated from a thin silver wire. The plot of voltage output against force (squares) falls on a straight line through the origin, indicating linearity. This plot was used to convert any sensor's voltage output into force. The g value of 9.8 µN mg^{-1} was used to convert weight to force.